Semiclassical calculation of bound states in a multidimensional system for nearly 1:1 degenerate systems

D. W. Noid and R. A. Marcus

Department of Chemistry, University of Illinois, Urbana, Illinois 61801 (Received 4 March 1977)

The method is devised to calculate eigenvalues semiclassically for an anharmonic system whose two unperturbed modes are 1:1 degenerate, by introducing a curvilinear Poincaré surface of section. The results are in reasonable agreement with the quantum ones. The classical trajectories also frequently show a large energy exchange among the two unperturbed normal modes. Implications for Slater's theory of unimolecular reactions, which neglects this effect, and for "quantum ergodicity" are described.

I. INTRODUCTION

In previous papers, semiclassical methods^{1,2} were developed in this laboratory for obtaining eigenvalues of bound state systems not permitting separation of variables. These methods utilized classical trajectories. More recently other quite different methods (perturbative-iterative) have also been developed. ³⁻⁵ In all but Ref. 2(c) and 6 the systems treated had two anharmonically coupled oscillators whose unperturbed frequencies were incommensurate. There was, as a result, little energy transfer between the two degrees of freedom. When the unperturbed frequencies become commensurate, considerable energy sharing begins to occur.

Recently, we have treated systems where the unperturbed frequencies are equal, ⁶ and the results are described in the present paper. It is shown how eigenvalues can be calculated semiclassically by introducing the concept of a curvilinear Poincaré surface of section, as well as by a "trajectory closure method," which joins the ends of a trajectory using a rectilinear Poincaré surface of section.

The present results also bear on other topics, such as Slater's assumption, ⁷ in his harmonic treatment of unimolecular reactions, that degenerate vibrations played a special role, with no energy sharing, and a suggestion in the literature that a "quantum ergodicity" ⁶⁻¹⁰ describes some features of resonant systems such as the present one. The present results are used to examine both of these.

II. HAMILTONIAN AND TRAJECTORIES

The Hamiltonian used is the treatment of this 1:1 resonance is the usual Henon-Heiles¹¹ one used extensively in the literature of anharmonically coupled oscillators.

$$H = \frac{1}{2}(p_x^2 + p_y^2 + x^2 + y^2) + \lambda x(y^2 - \frac{1}{3}x^2), \qquad (2.1)$$

where x and y are the oscillator (or normal mode) coordinates, p_x and p_y are the canonically conjugate momenta, and λ is an anharmonic coupling constant. If polar coordinates are introduced, by setting x and y equal to $r\cos\theta$ and $r\sin\theta$, the Hamiltonian becomes

$$H = \frac{1}{2}(p_r^2 + r^2 + p_\theta^2/r^2) - (\frac{1}{3}\lambda r^3)\cos 3\theta . \tag{2.2}$$

When the classical equations of motion arising from the Hamiltonian (2.1) or (2.2) are integrated numerically, we find that two classes of trajectories are obtained, depending on the initial conditions, as in Figs. 1–3. They may be termed "librating" and "precessing" type trajectories and correspond to different amounts of average internal angular momentum in (x, y) space. In Fig. 1 are three librating trajectories, labeled A, B, and C, each obtained by successive 120° rotations in the (x, y) plane. The trajectories in Figs. 2 and 3 are single ones and are of the precessing type, the one in Fig. 3 having more internal angular momentum than that in Fig. 2.

To understand the types of trajectories in Figs. 1-3, and ultimately apply quantum conditions, the semiclassical treatment of the unperturbed system will first be considered in the next section.

III. TRAJECTORIES AND SEMICLASSICAL QUANTUM CONDITIONS FOR THE UNPERTURBED SYSTEM

When the internal angular momentum of this system is nonzero, the unperturbed trajectory is a periodic one, an ellipse. (It degenerates into a straight line passing through the origin in the case of zero angular momentum.) The unperturbed semiclassical wavefunction is constructed from a family of these ellipses, each member of the family being obtained by a suitable rotation of this ellipse about the origin. Members of the family are given in Fig. 4. There are inner and outer concentric

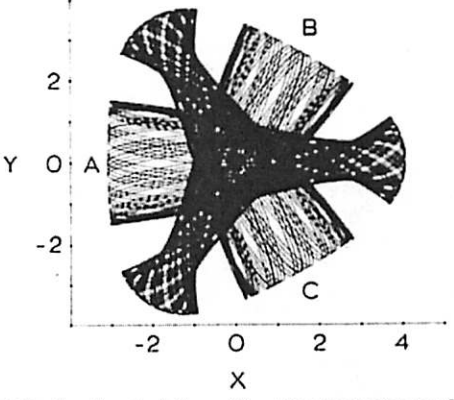


FIG. 1. A set of three librating trajectories for the Hamiltonian (2.1), with E=6 and $f_x=0.9650$. Trajectories B and C are obtained by successive 120° rotation of the initial conditions for trajectory A, starting in each case at x=0, y=0.

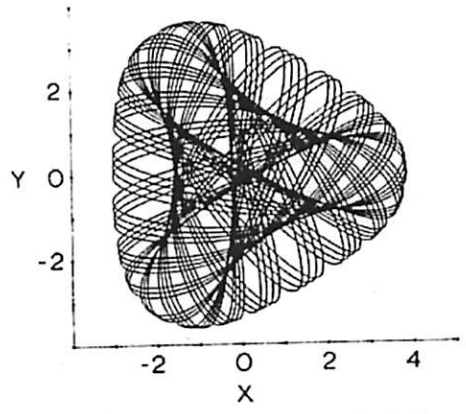


FIG. 2. Example of a precessing trajectory with low average angular momentum l, for the Hamiltonian (2.1) with E=6 and $f_x=0.6000$.

circles there, which are envelopes of the curves in the family, and which form the two caustics. Each point within the annulus bounded by the two concentric circles lies on some trajectory of the family, while points outside this annular region do not. The wavefunction is large within the annulus bounded by the two caustics and is exponentially vanishing outside.

We proceed to apply the quantum conditions. By integrating along a circle in the annulus (e.g., path A in Fig. 4) and concentric with the above pair, one proceeds along a path crossing neither caustic. The phase change of the semiclassical wavefunction on completing one such cycle around the origin is $\mathfrak{S}p_{\theta}d\theta$ (in units of \hbar = 1), evaluated at a given r. It must equal $2\pi l$, where l is an integer, in order that the wavefunction be single valued. That is,

$$\oint p_{\theta} d\theta = 2\pi l \quad . \tag{3.1}$$

Furthermore, evaluation of a phase integral $f(p_x dx + p_y dy)$ along any topologically equivalent path (path which touches or encloses the same number of caustics, zero in the present case) must have the same value, $2\pi l$.

A second quantum condition can be obtained by integrating along a radius vector over one cycle between the

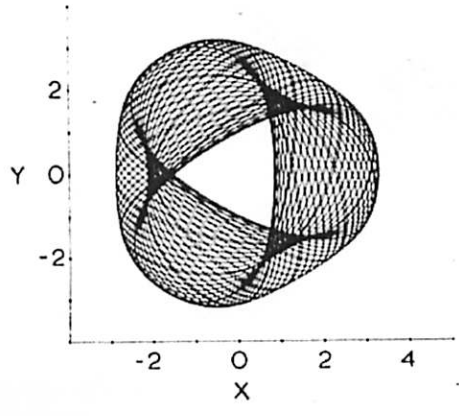


FIG. 3. Example of a precessing trajectory with high l, when the Hamiltonian is (2.1) with E=6 and $x_0=0.8500$.

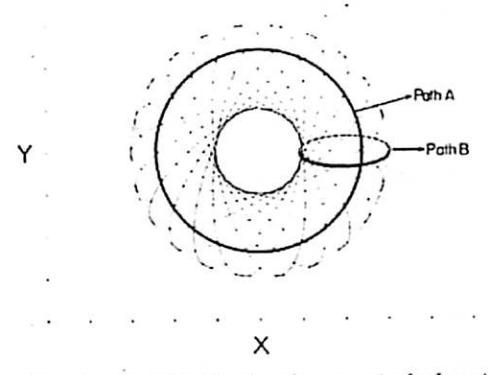


FIG. 4. Trajectories for the unperturbed system [Eq. (2.1) with $\lambda=0$] with finite *l*. Inner and outer concentric circles about the origin form the caustics. Path *A* is used for (3.1) and path *B* for (3.2).

two concentric circles (caustics); the phase integral equals $\mathfrak{sp}_r dr$ (path B in Fig. 4). The path encloses or touches two caustics, with a phase $loss^{12}$ of $\frac{1}{2}\pi$ at each. The net phase change is thus $\mathfrak{sp}_r dr - \pi$, and must equal $2\pi n_r$, where n_r is an integer, to achieve single valuedness of the semiclassical wavefunction. Thus,

$$\oint p_r dr = 2\pi (n_r + \frac{1}{2}) . \tag{3.2}$$

Instead of (3.2) one could also have used the following condition, use of which is also made later; the trajectory along an ellipse in Fig. 4 touches a caustic four times, and so there is a loss of phase of $(4\frac{1}{2}\pi)$. The net phase change should equal $2\pi n$, where n is an integer. The phase integral change along the trajectory, $f(p_x dx + p_y dy)$, is the sum of two r-cycle phase integrals $2fp_r dr$ and a θ -cycle one $fp_\theta d\theta$, since two r-cycles and one θ -cycle are completed. Thus,

$$\oint_{\text{traj}} (p_x dx + p_y dy) = 2 \oint p_\tau dr + \oint p_\theta d\theta = 2\pi (n+1) . \tag{3.3}$$

The second half of Eq. (3.3) can also be obtained from (3.1) and (3.2), with

$$n = 2n_r + l \quad , \tag{3.4}$$

so Eq. (3.3) is not independent of them. n is seen to be even or odd according as l is even or odd. The energy for the unperturbed system depends only on n.

When the angular momentum p_{θ} is zero, the periodic trajectory along the ellipse degenerates as already noted into an oscillation along a straight line passing through the origin [cf. Eq. (2.2) with p_{θ} and λ both zero]. The family of trajectories used to construct the wavefunction is now a family of straight lines, all intersecting at the origin. There is one envelope of the family—a circle concentric with the origin and composed of the turning points of the straight line trajectories. There is also now one focus—the intersection point of all the trajectories, namely, the origin. Integrating along a path at constant r, one again obtains (3.1), but now with l=0, since p_{θ} is zero for all members of the family. Integrating along one of the straight line trajectories from one extremity to the other and back, the cyclic path integral

now equals $2 \int p_r dr$, where $\int p_r dr$ denotes the path integral from the origin to the outer extremity and back. The loss of phase along this path as a result of touching two caustics (the endpoints) is $2(\frac{1}{2}\pi)$ and as a result of passing through the focus¹² is π . The net phase change is therefore $2 \int p_r dr - 2\pi$. This result should equal $2\pi n$ where n is an integer, in order that the semiclassical wavefunction be single valued. Thereby, one again obtains the second half of (3.3), but now along a straight line trajectory and now with l=0.

IV. SEMICLASSICAL QUANTUM CONDITIONS AND RESULTS

A. General

It was noted in Sec. II that there are two classes of trajectories. Those depicted in Figs. 2 and 3 involve precessions of the unperturbed ellipses, while those depicted in Fig. 1 merely involve libration of the ellipses, due to the system's having smaller internal angular momentum. As already remarked, there are three equivalent librating trajectories, differing by 120° in their orientation. Thus, a family of highly eccentric ellipses in a low angular momentum unperturbed system (or of straight lines when l=0) evolves into a collection of three librating trajectories in the perturbed case. The surface of section method for calculating eigenvalues, introduced in the previous paper, l=0 is again employed.

It is recalled that a conventional (i.e., planar) Poincaré surface of section for y=0 is one which gives the trajectory values of p_x and x at y=0, for $p_y>0$ or, instead, for $p_y<0$. Introduced in the present paper is the notion of a curvilinear surface of section. Using curvilinear coordinates (ξ,η) one records on the curve $\eta=$ constant the values of p_t and ξ each time the trajectory crosses that curve, for $p_\eta>0$ or, instead, for $p_\eta<0$. Similarly, one can introduce a curvilinear section having $\xi=$ constant. In this paper, ξ and η are chosen to be the polar coordinates τ and θ . A surface of section $\tau=\tau_0$ for a precessing trajectory is given in Fig. 5 and for three librating trajectories in Fig. 6.

The four caustics associated with each librating trajectory in Fig. 1 are the four envelopes enclosing each

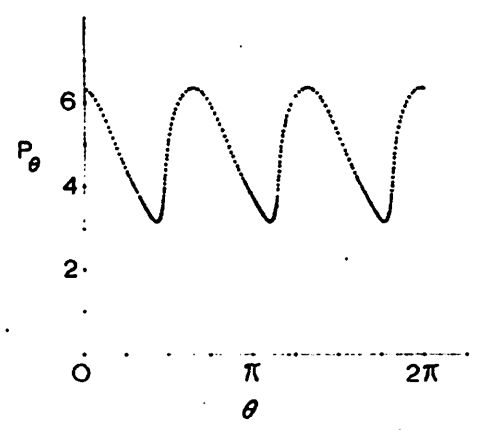


FIG. 5. A surface of section $r = r_0(=\sqrt{7})$ for a precessing trajectory for system (2.1) for $p_r < 0$, for the trajectory in Fig. 3.

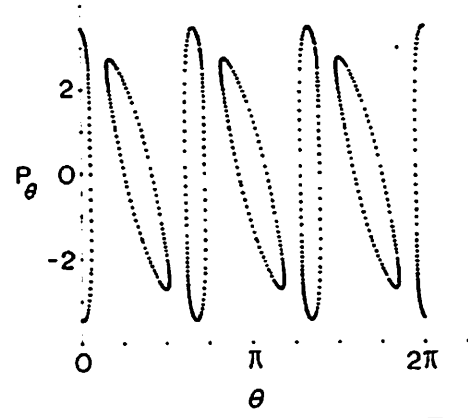


FIG. 6. A surface of section at $r = r_0 (= \sqrt{7})$ for the three librating trajectories in Fig. 1, for $p_r > 0$.

librating trajectory. The caustics associated with the precessing trajectories in Figs. 2 and 3 are shown in Fig. 7(a) and 7(b), respectively. There is an outer somewhat circular caustic and an inner caustic, the curve B'E'BE'B'E, which has six cusps. The manner in which this cusped caustic evolves from the caustics of the librating trajectories is described in Sec. VII.

B. Precessing trajectories

There are two topologically independent closed paths in Fig. 7, one a circular like path between the two caustics (similar to path A in Fig. 4) and the other a path joining the inner and outer caustics, such as path B in Fig. 7(b). (The same path can be used for Fig. 7(a) also since the caustics E''B and B'E don't interfere with BE'B''E. The trajectories which touch the former have a sign of p_y at y=0 opposite to that of trajectories which touch the latter.)

The quantum conditions for these precessing trajectories are readily given. Corresponding to Eq. (3.1) on an $r=r_0$ surface of section, where r_0 is conveniently chosen to lie between the inner and outer caustics, one has

$$\int p_{\theta} d\theta = 2\pi l \quad . \tag{4.1}$$

The second quantum condition, appropriate to path B

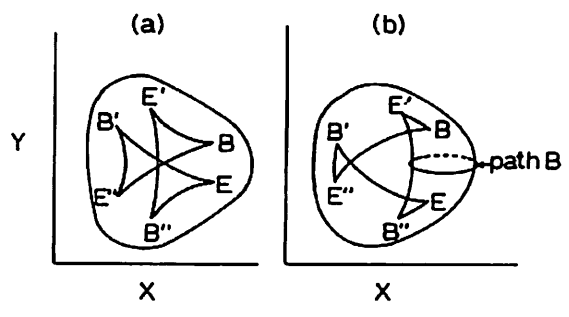


FIG. 7. Caustics associated with two precessing trajectories, Fig. 7(a) corresponding to Fig. 2 and 7(b) to Fig. 3. In each case the inner caustic is the cusped curve B"E"BE"BE. The outer caustic is the outer closed curve.

in Fig. 7, is obtained from (3.2). Eq. (3.2) is used as the second phase integral: A surface of section y=0 is selected at $\theta=0$, and for it the phase integral $\mathcal{F}p_rdr$ equals $\mathcal{F}p_xdx$. The second quantum condition is therefore

TABLE I. Comparison of semiclassical and quantum mechanical eigenvalues for hamiltonian (2.1).

			7-i	Camiologgical	Quantum	
State (i,n)	E ⁰	Sym	Polar quantum (present)	Semiclassical (present)	Rice et al. 8	"Type"
0,0)	1.0	A	0.9986	0.9947	0,998	HL
± 1, 1)	2.0	E	1.9901	1,9863	1.990	HL HL
0, 2)	3.0	A	2.9562	2.9506	2.956	G
± 2, 2)	3.0	E	2.9853	2.9815	2,986	HL G
(± 1, 3)	4.0	E	3.9260	3,9233	3,926	~ L ~ L
(± 3, 3)	4.0	A	3.9824 3.9858	3,9803	3.982 3.986	~ L ~ L
(0, 4)	4.0	A	4.8702	4.8573	4,870	O
(+ 2, 4)	5.0	E	4.8987	4,8954	4.898	G M
(± 4, 4)	5.0	E	4.9863	4.9821	4.986	G ~ L
(t 1,5)b	6.0	E .	5.8170	5.816	5,818	~ L ~ L
(± 3, 5)	6, 0	A	5.8670 5.8815	5.8713	5.868 5.882	M M
(£ 5, 5)	6.0	E	5, 9913	5.9869	5.991	~ L
(0,6)	7.0	Α	6.7379	6,7078	6.744	G
(t 2, 6)	7.0	E	6.7649	6.7709	6,770	G M
(± 4, 6)	7.0	E	6, 8354	6.8500	6,857	M ~G
(± 6, 6)	7.0	A	6.9989 6.9994	6, 9958	7.001 7.002	~ L ~ (
(t 1, 7)b	8.0	E	7,6595	7,655	7.690	~ L ~ L
(± 3, 7)*	8.0	A	7.6977 7.7369	7.7178	7.736 7.745	M <i>M</i> ~
(± 5, 7)	8.0	Б	7.8327	7,8289	7.845	~ G ≈ L≈ (
(± 7, 7)	8.0	E	8,0094	8.6054	8,015	⇔ G M≈
(0, 8)	9,0	A	8.5541	8,4919	8.674	M
(± 2, 8)	9.0	. E	B. 5764	•••	8,693	≈ L M
(+ 4, 8)	9,0	E	8,6779	•••	8,771	M M
(£ 6, 8) ⁶	9.0	. A	8.8113 8.8152	8,8084	6, 877	G
(+ 8, 8)	9.0	E	9,0217	9,0151	•••	
(± 9, 9)	10.0	A	10,0354 10,0356	10,028	•••	
(0, 10)	11.0		10,3052	10, 1942	•••	
(± 10, 10) ^t	11,0	.	11.0497	11.0401	•••	

^aUnless otherwise stated all eigenvalues, apart from those for l=0, were calculated using Eqs. (4.1) and (4.2), as per text. The l=0 trajectories were treated by the straight line method using (3.3).

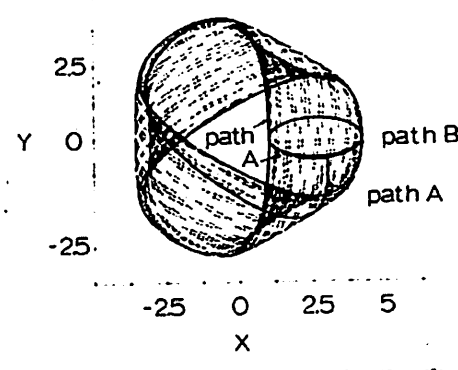


FIG. 8. Precessing trajectory for Hamiltonian (2.1), indicating a path A used in the trajectory closure method. It contains one cycle of the near-cllipse motion, and has E=10, $x_0=1.0000$.

$$\oint p_r dr = \oint p_x dx = 2\pi (n_r + \frac{1}{2}).$$
 (y = 0

For a somewhat easier evaluation of the integral, care was exercised to ensure that the circular section $r=r_0$ for evaluating $fp_\theta d\theta$ does not pass through the sixcusped caustic region evident for precessing trajectories in Fig. 7. In the 18 precessing cases considered in the present paper, corresponding to 18 eigenvalues (or to 24 including near degeneracies), it was easy to find such an $r=r_0$ surface of section in all cases but three. For those three cases, noted in Table I, a "trajectory closure method" was developed: After one cycle of a near-ellipse trajectory the system returns to the same neighborhood of the initial point, as in Fig. 8. For the same θ of the final and initial point the new r might differ from the original r by about one unit, in the units of the present figures. After this cycle the ends of the trajectory are then joined on a θ = constant surface of section (e.g., on the y=0 surface of section at $\theta=0$ in Fig. 8.) The phase integral was then computed along the trajectory and along the link connecting the trajectory ends on the surface. 13,14 (The surface of section data was obtained from many cycles of the trajectory, as before.) The expression used for this eigenvalue, taken from Eq. (3.3), is

$$\oint_{1\pi a^{3}} (p_{x}dx + p_{y}dy) = 2\pi n + \frac{1}{2}C\pi \quad (1 \text{ cycle}), \qquad (4.3a)$$

where n is the principal quantum number, traj indicates integration along the trajectory, and C is the number of times each cycle touched a caustic

$$C = 4$$
 . (4.3b)

One could have used (4.3) and (4.2), instead of (4.1) plus (4.2), for the remaining 15 precessing trajectories. The computational time is approximately the same and the results are of similar accuracy. An example is given later.

C. Librating trajectories

In the case of the librating trajectories, all three librating trajectories (each obtained from one of them by successive 120° rotations as in Fig. 1) contribute to construction of a suitable wavefunction, but data on only

These trajectories were treated using Eqs. (4.1) and (4.3) in the three precessing cases $\{(\pm 3,7), (\pm 6,8), (\pm 10,10)\}$, and using (4.4) and (4.3) in the two librating cases $\{(\pm 1,5), (\pm 1,7)\}$.

one is needed, because of the C_3 symmetry of the Hamiltonian (2.2).

We consider first the main quantum condition determining the energy. In the unperturbed case the energy is determined by the principal quantum number n, which is obtained in (3.3) from the phase integral along the trajectory. Just as (3.3) was adapted via the "trajectory closure method" to the precessing case in the form of (4.3), (4.3) can be again used for the librating case. For example, for trajectory A in Fig. 1 the ends of the trajectory were joined after one near-ellipse cycle, by connecting them on the x=0 surface of section.

The second quantum condition is obtained using the coalescence of caustics discussed in Sec. VII. It is illustrated there that the phase integral $\int p_{\theta}d\theta$ continues smoothly from the librating case of the precessing one. apart from the fact that because of the librating the value of \$p_d\theta summed over all three librating trajectories is twice as large as the spade from a single precessing trajectory, i.e., equals $2(2\pi l)$. Using this continuity Eq. (3.1) was adapted to the librating case: Even when the libration was quite large, I was still fairly close to zero. To adapt (3.1) to the librating case, it was first observed that $\int p dy$ on the x=0 surface of section for trajectory A in Fig. 1 equals one-half $fp_{\theta}d\theta$ for trajectory A, since two θ intervals contribute equally to $\int p_a d\theta$. Thus, this $\int p_a dy$ equals one-sixth the sum of \$p_d\theta for all three trajectories, i.e., one-sixth of $2(2\pi l)$. Then, the second quantum condition for the librating case is

$$\oint p_{y}dy = \frac{1}{3}2\pi l$$
 (Fig. 1, trajectory A, x = 0). (4.4)

This adaptation of (3.1) to yield (4.4), aimed at yielding single valuedness of the semiclassical wave function as one makes a single circuit around the origin on an $r=r_0$ path, is an approximate one: Along this path p_0 is complex valued in the θ intervals between the caustics of the trajectories in Fig. 1. Equation (4.4) neglects the effects of such contributions from these θ -forbidden intervals. Improvements would entail their inclusion and use of a suitable connection formula. 15-17 Fortunately, the energy of a librating trajectory in the "nearly degenerate" case is not very sensitive to $f p_{\theta} d\theta$, i.e., to l, being mainly dependent on the principal quantum number n. For example, the energy of a librating trajectory changed by only one part in 500 when the l defined by (4.4) was changed from 0 to $\frac{1}{2}$ holding the *n* defined by (4.3) constant. Two of the eight librating trajectories had $l=\pm 1$. The remaining six librating trajectories had a smaller l, and l was chosen to be zero. within the approximation embodied in (4.4), by simply choosing a straight line trajectory and using (3, 3). Ultimately another trajectory and a connection formula15-17 should be used.

V. NUMERICAL PROCEDURES

The initial conditions (f=0) employed in generating most precessing type trajectories were $x(0)=x_0$, $y(0)=p_x(0)=0$. $p_y(0)$ was determined from these initial conditions and the total energy. The librating trajectories

and the very low l precessing trajectories were started at the origin [x(0)=y(0)=0], and the other initial conditions chosen for them involved the values of $p_x(0)$ and E: A value for E and for $f_x = \frac{p_x^2(0)}{p_x^2(0)} + \frac{p_y^2(0)}{p_y^2(0)}$ was selected, $p_x^2(0) = \frac{p_x^2(0)}{p_x^2(0)}$ and $p_y^2(0) = \frac{p_x^2(0)}{p_x^2(0)}$ were found from energy conservation.

To obtain points on the Poincaré surface of section for $r=r_{0}$, for both types of trajectories, a linear interpolation of two points along the trajectory on either side of the surface was used. A surface of section for $r=r_{0}$ was shown in Fig. 5 for the precessing trajectory of Fig. 2 and in Fig. 6 for the three librating trajectories of Fig. 1. A phase integral was calculated from the points on a surface of section, using a three-point integration formula for nonequally spaced points. (The accuracy of the integration was checked by integration using a larger number of points. All integrations were performed using an IBM 360-75 computer and FORTRAN.)

The trajectory closure method, used for the two precessing and two librating states noted in Table I, was executed as already stated, by following one cycle of the near-ellipse trajectory, joining the ends along a y=0 surface of section, and using (4.3) and (4.2) or (4.3) and (4.4). The iteration procedure to obtain E and x(0) was the same as described previously. ¹⁶ Results obtained with the trajectory closure method agreed with those obtained with the two surfaces of section. ¹⁹ Use of the straight line trajectories to obtain the l=0 "librating" trajectory and eigenvalue was straightforward, using (3.3).

VI. QUANTUM MECHANICAL EIGENVALUES

The basis set of wavefunctions used to calculate the eigenvalues by a variational method were eigenfunctions of the unperturbed Hamiltonian H_0 and, expressed in terms of polar coordinates, are designated as $\psi_{n,l}^0(r,\theta)$. The potential in H_0 depends on r but not on θ . In units such that n=1 and that the vibration frequency ω is unity, the energy is n+1 and the unperturbed Schrödinger equation is

$$H_0 \psi_{ni}^0 = \left(-\frac{1}{2} \frac{\partial^2}{\partial r^2} + r^2 - \frac{1}{2r^2} \frac{\partial^2}{\partial \theta^2} \right) \psi_{ni}^0 = E \psi_{ni}^0 = (n+1) \psi_{ni}^0 , \qquad (6.1)$$

where n is the principal quantum number, $0, 1, \ldots$. These ψ_{nl}^0 were chosen to be eigenfunctions of the angular momentum operator p_0 , where l=0, and to be real-valued linear combinations²⁰ of the p_0 eigenfunctions for $\pm l$, when $l \neq 0$. Since l goes from -n to n in units of 2, there is a degeneracy of n+1 in the unperturbed system.

The perturbation is H_1 ,

$$H_1 = -(\frac{1}{3}\lambda r^3)\cos 3\theta = -\frac{1}{6}\lambda(x_+^3 + x_-^3)$$
, (6.2)

where 20

$$x_{\lambda} = x \pm iy = r \exp(\pm i\theta) . \tag{6.3}$$

The matrix elements²⁰ $\langle nl | H_1 | n'l' \rangle$ are found to be

$$\langle nl \mid H_1 \mid n'l' \rangle = -(\lambda/6) \sum_{i,i+a3} A_1^a \delta_{n,m'+3} + A_2^a \delta_{n,m'+1} + A_3^a \delta_{n,m'-1} + A_4^a \delta_{n,m'-3} ,$$
 (6.4)

where the sum \sum indicates a sum involving only the upper signs, plus a sum involving only the lower signs. The A_i^{ab} are given by

$$A_{1}^{a} = \mp \left[\frac{1}{6}(n' \pm l' + 2)(n' \pm l' + 4)(n' \pm l' + 6)\right]^{1/2},$$

$$A_{2}^{a} = \pm 3\left[\frac{1}{6}(n' \mp l')(n' \pm l' + 2)(n' \pm l' + 4)\right]^{1/2},$$

$$A_{3}^{a} = \mp 3\left[\frac{1}{6}(n' \mp l' - 2)(n' \mp l')(n' \pm l' + 2)\right]^{1/2},$$

$$A_{4}^{a} = \pm \left[\frac{1}{6}(n' \mp l' - 4)(n' \mp l' - 2)(n' \mp l')\right]^{1/2}.$$
(6.5)

The program for the variational calculation of the eigenvalues was written in double precision, using basis sets of 406 and 595 elements to test convergence, 21 and using a matrix diagonalization package EISPAC. 22

The Hamiltonian (2.2) and its quantum mechanical counterpart, Eq. (6.1) belong to the point group C_3 with respect to rotation of θ . As such, each eigenvalue is either A type and is nondegenerate or is E type and is doubly degenerate, the former being for the states labeled $l=0,\pm 3,\pm 6,\pm 9,\ldots$ in Table I and the latter being for states labeled $l=\pm 1,\pm 2,\pm 4,\pm 5,\ldots$. The perturbation in (1.2) couples unperturbed states which differ in l by multiples of 3, and so couples $l=\pm 3$ states with each other (and with $0,\pm 6$, etc.), thus removing their degeneracy, and similarly for the $l=\pm 6$ states, etc. (The l=0 states were nondegenerate to begin with.) The ± 2 states, etc., are not coupled by the perturbation and their degeneracy is not removed.

VII. RESULTS AND DISCUSSION

The semiclassical and quantum results are given in Table I. (The value of λ chosen was such as to permit comparison with the results in Ref. 8, and thereby to analyze the quantum ergodicity discussed therein.) The results are seen to agree to about 1/1000 at the higher energies and to about 1/500 at the lower ones. Further analysis, as discussed in Sec. IV, using a suitable connection formula, would be needed to treat the splitting of the levels 15-17: in the librating region the caustics to be "connected" are real, and in the precessing region they are complex valued. The threefold symmetry couples traveling waves of opposite l, when $l=\pm 3, \pm 6...$, breaking the degeneracy of those states.

In Table I a comparison of the quantum results is also given with the quantum results of Rice and co-workers, ⁸ who used Cartesian coordinates instead of polar ones. (The conversion of their units to ours is given in Appendix.) The two sets of quantum results agree well for

energies below 7.0. At higher energies a divergence sets in, being largest for the state $(\pm 6, 8)$, amounting to 64/9000, while the present semiclassical agrees with the present quantum result to 5/9000. At higher energies the restricted Cartesian basis set is probably not adequate, a point to be returned to later.

At low energies the trajectories are quasiperiodic (they yield regular patterns in the Poincaré surfaces of section), and so the present semiclassical method can be used to calculate eigenvalues. At higher energies, the patterns on the Poincaré surface of section become shotgunlike, first near the separatrices in the surface of section (separatrices separate resonant centers)24 and then, at high enough energies, everywhere. The stablest trajectories with the greatest propensity to remain quasiperiodic as the energy is increased are those near the resonant centers25 (see Fig. 9). For this reason one finds that at the higher energies it is still possible to calculate some eigenvalues semiclassically, namely those associated with trajectories passing near a resonant center. For example, although there were no stable trajectories for the states $(\pm 2, 8)$ and $(\pm 4, 8)$, with an n of 8, semiclassical eigenvalues for some other states could be calculated at n=8, 9, and 10 even though there were regions of nearby instability.

The present results can be used to examine the suggestion of "quantum ergodicity" in this system⁸⁻¹⁰: It was noticed previously⁸⁻¹⁰ that at higher energies the coefficients in the linear combination of unperturbed wavefunctions used to represent the wavefunction showed a type of "global" behavior, i.e., a substantial components' overlap between adjacent levels differing only in n_x quantum number at given (n_x+n_y) , i.e., at given n. The behavior reflected, it was believed, either a "quantum ergodicity" or an unhelpful choice of basis set, e.g., Cartesian rather than polar. One can now obtain insight into the origin of the phenomenon.

The problem of using a truncated Cartesian coordinate basis set is reflected in the eigenvalue 2.986 where one of the doubly degenerate E levels was labeled as HL (highly local) and the other was labeled as G (global) (cf.

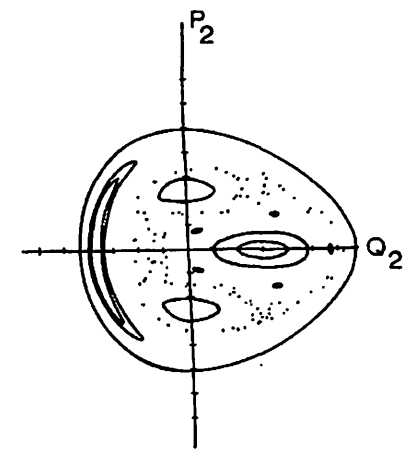


FIG. 9. Surface of section at x=0 for the system (2.1) showing the resonance centers, at E=10 in our units, taken from Ref. 22.

Table I) even though the use of polar coordinates in the present paper shows that the behavior in this respect should have been actually identical if an untruncated Cartesian basis set had been used. This difficulty occurred frequently with the Cartesian basis set, e.g., in about one-half the cases of the degenerate E states in Ref. 8.

Actually, the present study shows that the large majority of eigenvalues are associated with quasiperiodic trajectories rather than erogidic ones. Thus, instead of an ergodicity the phenomenon termed "quantum ergodicity" largely reflects the extensive (but essentially periodic) energy exchange between the two degrees of freedom. Use of a polar rather than Cartesian basis set would yield unperturbed quantum numbers n and l less apt to change their values than n_x and n_y during the motion.

Recently, after completion of the present work, 6 a semiclassical method was presented by Sorbie and Handy2(c) for calculating eigenvalues in the present system with the x^3 term in (2.1) absent. The method, whose derivations2(c) tacitly assume separation of variables, 26 is a variant of the trajectory method developed earlier in this laboratory1,2; Sorbie and Handy continue the trajectory until it almost closes on itself, and then they evaluate two independent phase integrals. Trajectories were about three times as long as the present ones, and corresponded, in the unperturbed case, to numbers n_x and n_{u} in the range 0-2. (They considered trajectories which pass through the origin.) One cannot readily compare the calculation in other respects. We have been able to derive the equations of Ref. 2(c) under an approximation milder than separation of variables, though of uncertain accuracy. 27

The question of relative computation times of quantum mechanical and semiclassical methods is of interest. In the present case where the matrix elements can be evaluated analytically the former is faster for the system treated using our present computational software.

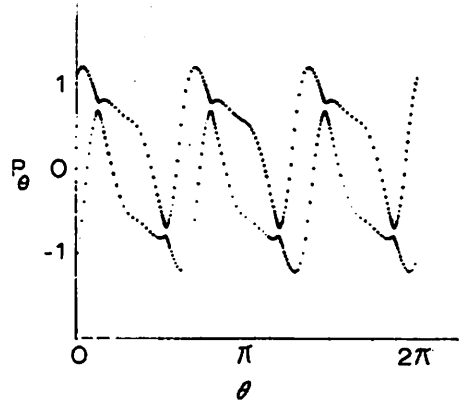


FIG. 10. Surface of section at $r=r_0=\sqrt{5}$ for two precessing trajectories which are near the precessing-librating boundary (cf. Fig. 11). E=3 and $f_x=0.435$. [The lower curve was actually obtained from the trajectory responsible for the upper one, by rotating the initial conditions by 60° in the (x,y) plane, so as to change the sign of the initial P_2 and still have $p_r>0$.]

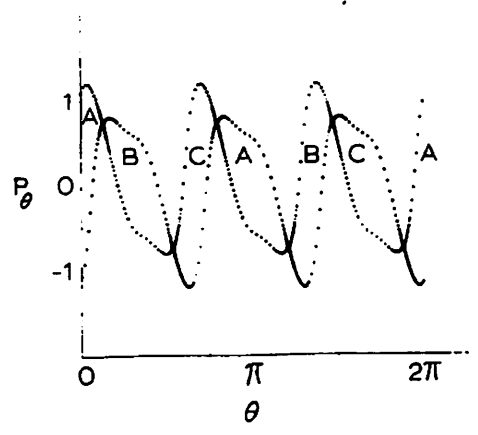


FIG. 11. Surface of section at $r=r_0=\sqrt{5}$ for three librating trajectories A, B, C which are identical apart from 120° rotations and which are near the precessing-librating boundary. Each trajectory forms two lobes, as indicated. E=3 and $f_x=0.434$ for trajectory B.

When analytical evaluation is not possible, it is expected that the semiclassical method will be faster for vibrationally excited states. The computer time needed is mainly for the trajectory itself. The time for obtaining the surfaces of section and for evaluating the integrals is negligible.

We comment briefly on an implication 28 of the present results for Slater's unimolecular reaction rate theory. Stater assumed in his harmonic oscillator treatment that any (unperturbed) degenerate modes remained degenerate throughout the decomposition of a single molecule. Thus, his phase-averaged amplitude-averaged dissociation rate constant for a molecule of given energy varied as the (n-1)th power of the excess energy (E $-E_0$), where n was, because of assumed degeneracy, less than the number of vibrational oscillators: A degenerate system occupies a smaller-dimensional region of phase space than the total number of dimensions, even when integrated over phases and amplitudes. However, the present results show that anharmonicity readily introduces energy sharing among modes formerly degenerate in the unperturbed system, even in the quasiperi-

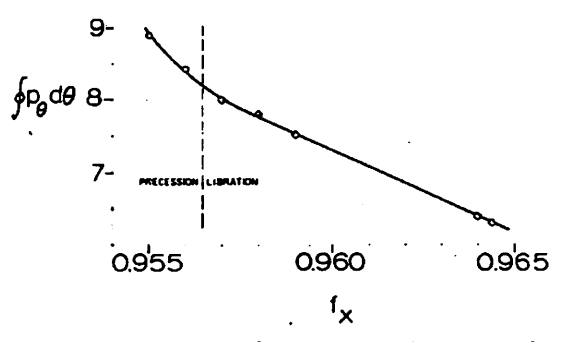


FIG. 12. Continuation plot of $\mathfrak{sp}_{\theta}d_{\theta}$ for librating and precessing trajectories. $\mathfrak{sp}_{\theta}d\theta$ for the precessing trajectories is the actual value while $\mathfrak{sp}_{\theta}d\theta$ for the libration cases is the sum over all three equivalent librating trajectories, divided by a factor of two (cf Eq. (7.1)].

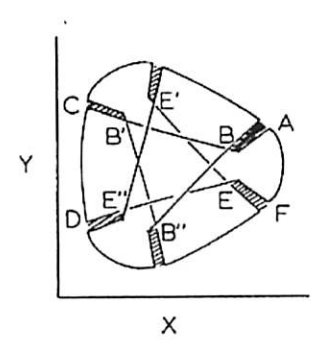


FIG. 13. Caustics of three librating trajectories, fairly near the librating-precessing boundary. The caustics bounding the shaded regions will coalesce, and others such as E''E' and B''B will split and reform as B''E' and E''B', when a precessing trajectory is formed,

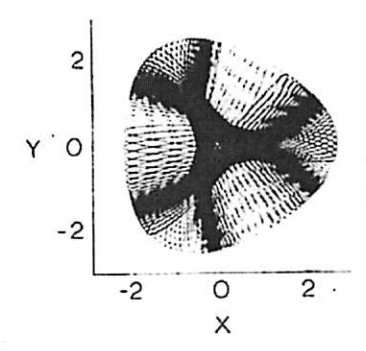


FIG. 15. A precessing trajectory near the precessing-librating boundary. Its surface of section is given in Fig. 10.

odic regime, and so this particular result of Slater theory is in error. (Among other approximations there is also the harmonic oscillator approximation itself.) This energy sharing among degenerate modes, evident too in some recent trajectory calculations for high energy molecules, ²⁹ is a periodic (quasiperiodic) one, and is to be distinguished from an ergodic-type energy sharing which would occur among all coupled modes at sufficiently high energy.

We consider next the coalescence of caustics. In Fig. 10, a p_{θ} vs θ Poincaré surface of section is given (the upper curve in Fig. 10), for a precessing trajectory with an initial condition close to that for a precessing-librating boundary. A second precessing trajectory having an initial p_{θ} of opposite sign is also given (the lower curve in Fig. 10).

In Fig. 11 is given a p_{θ} vs θ plot for a trajectory with an initial condition only very slightly different from that in Fig. 10, but such that the trajectory has become a librating one. Using the fact that the lower curve in Fig. 10, is obtained from the upper one by a 180° rotation, one can show that the p_{θ} d θ for the precessing trajectory goes over to one-half the value of p_{θ} d θ in the librating case, as in (7.1), and leads to Eq. (4.4).

$$\oint_{-\infty} p_{\theta} d\theta - \frac{1}{2} \oint_{-\infty} p_{\theta} d\theta .$$
(7.1)

A numerical demonstration of this result is given in Fig. 12.

We conclude with a description of the evolution of the caustics at the librating-precessing transition, including the formation of the inner six-cusped caustic in Figs. 2 and 3. In Fig. 13 are three equivalent librating trajectories fairly near the librating-precessing transition. At the transition the portions of the caustics

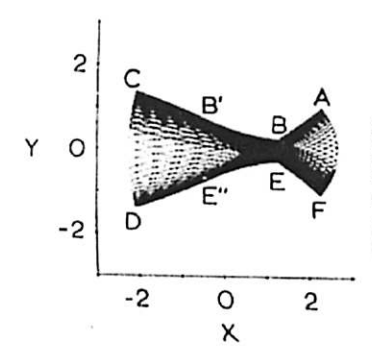


FIG. 14. A librating trajectory near the precessing-librating boundary. Its surface of section is given in Fig. 11 and labeled A there.

bounding the six shaded regions coalesce and disappear. Further, pairs of portions of caustics, such as E"E' and B'B, which cross when the trajectories are of the librating type, will split and reform new caustics B'E' and E"B' (and similarly for the other two pairs), when the trajectories become precessing ones, thereby developing into the six-cusped caustic of Fig. 7(a). Figure 14 gives a librating trajectory almost on the point of becoming a precessing one. The incipient formation of new caustics B''E' and E''B' is evident. In Fig. 15 is the precessing trajectory to which the librating trajectory of Fig. 14 has evolved. The old and the new caustics are all seen, some of which will disappear on one side of the librating-precessing transition and others of which will disappear on the other side, as one moves away from the transition point, by changing f_r .

APPENDIX. CONVERSION OF UNITS

To make a comparison of eigenvalues calculated in Ref. 8 with those calculated here the Hamiltonian used there was rescaled so as to agree with ours. The correspondence in eigenvalues is thus obtained by dividing the values in Ref. 8's Table V by 0.0125. The argument is given below.

The Hamiltonian in Ref. 8 is given by \overline{H} :

$$\overline{H} = -\left(\frac{\hbar^2}{2\mu}\right)\left(\frac{\partial^2}{\partial \overline{x}^2} + \frac{\partial^2}{\partial \overline{y}^2}\right) + \left(\frac{1}{2}\mu\omega^2\right)(\overline{x}^2 + \overline{y}^2) + \overline{x}\,\overline{y}^2 - \frac{1}{3}\overline{x}^3 \quad , \quad (A1)$$

where $\hbar\omega$ = 0.0125, $\,\mu$ = 1 and ω = 1. (In Table V of Ref. 8 $\hbar\omega$ is inadvertently written as 0.00125.) Introducing into (A1),

$$x = \alpha \overline{x}, \quad y = \alpha \overline{y}$$
 (A2)

where α is to be chosen, (A1) becomes (with $\mu = \omega = 1$)

$$\overline{H} = -\left(\frac{1}{2}\pi^2\alpha^2\right)\left(\frac{\theta^2}{\theta x^2} + \frac{\theta^2}{\theta y^2}\right) + \left(\frac{1}{2\alpha^2}\right)(x^2 + y^2) + \left(\frac{1}{\alpha^3}\right)(xy^2 - \frac{1}{3}\overline{x}^3). \tag{A3}$$

The Hamiltonian used in Eq. (2.1) is

$$H = -\left(\frac{1}{2}\right) \left(\frac{\partial^2}{\partial x^2} + \frac{\partial^2}{\partial y^2}\right) + \frac{1}{2}(x^2 + y^2) + \lambda(xy^2 - \frac{1}{3}x^3) . \tag{A4}$$

Now choosing

$$\alpha^2 = 1/\pi = 1/0.0125$$
, (A5)

$$H = \hbar H$$
, $\lambda = \hbar^{1/2} = (0.0125)^{1/2}$. (A6)

¹R. A. Marcus, Discuss. Faraday Soc. 65, 34 (1973).

²(a) W. Eastes and R. A. Marcus, J. Chem. Phys. 61, 4301 (1974). (b) D. W. Noid and R. A. Marcus, J. Chem. Phys. 62, 2119 (1975). (c) A variant of this trajectory method was recently published by K. S. Sorbie and N. C. Handy, Mol. Phys. 32, 1327 (1976); cf. K. S. Sorbie, *ibid.* 32, 1577 (1976). The tacitly added approximation contained in this method is discussed below in Refs. 26 and 27. These two papers are referred to as I and II, respectively, in those references.

3(a) S. Chapman, B. Garrett, and W. H. Miller, J. Chem. Phys. 64, 502 (1976). (b) N. C. Handy, S. M. Colwell, and W. H. Miller, Faraday Discuss, Chem. Soc. (in press). L. C. Perceival and N. Pomphrey, Mol. Phys. 31, 917 (1976). ⁵An earlier method based on periodic trajectories [M. C. Gutzwiller, J. Math. Phys. 12, 343 (1971), cf. 8, 1979 (1967); 10, 1064 (1969); W. H. Miller, J. Chem. Phys. 56, 38 (1972)] was shown to yield too many eigenvalues, and to yield wrong ones, thereby, at will. 26 For a system of two coordinates, except in a degenerate case, one needs two conditions to calculate the eigenvalues while the periodic trajectories formalism contains only one. Gutzwiller's method has usefulness in calculating density of states [M. C. Gutzwiller, J. Math. Phys. 11, 1791 (1970); R. Balian and C. Bloch, Ann. Phys. 69, 76 (1972)]. An analysis is given by M. V. Berry and M. Tabor, Proc. R. Soc. London Ser. A 349, 101 (1976). A modification of Gutzwiller's method for eigenvalues is given in W. H. Miller, J. Chem. Phys. 68, 996 (1975).

⁶D. W. Noid, Ph. D. thesis, University of Illinois, Urbana, April 1976 (unpublished). [D. W. Noid, Diss. Abstr. Int. B 37, 2278 (1976)].

¹N. B. Slater, Theory of Unimolecular Reactions (Cornell University Ithaca, N. Y., 1959).

⁸K. S. J. Nordholm and S. A. Rice, J. Chem. Phys. 61, 203 (1974).

⁹K. S. J. Nordholm and S. A. Rice, J. Chem. Phys. 61, 768 (1974).

¹⁰K. S. J. Nordholm and S. A. Rice, J. Chem. Phys. **62**, 157 (1975).

¹¹For example, M. Henon and C. Heiles, Astron. J. 69, 73 (1964); G. Contopoulos and M. Moutsoulas, Astron. J. 70, 817 (1965); W. H. Jeffreys, Astron. J. 71, 306 (1965); B. Barbanis, Astron. J. 71, 415 (1966); G. H. Walker and J. Ford, Phys. Rev. 188, 416 (1969).

¹²J. B. Keller, Ann. Phys. 4, 180 (1958).

¹³In practice the phase integral was calculated by integrating the differential equation for the phase S, namely that \dot{S} equals $p_s\dot{x}+p_s\dot{y}$, where the dot denotes d/dt. The integration was along the trajectory and then along the link joining the ends of the trajectory.

¹⁴The precessing trajectory usually returned more closely to itself after three cycles than after one, and so a shorter path was needed for joining the two ends of the trajectory on the surface. When three cycles are used the value of $p_x dx + p_y dy$ integrated along the path equals, of course, three times the right hand side of (4.3a). The values of n obtained for the one cycle and three-cycle paths were the same.

¹⁵M. S. Child, Discuss. Faraday Soc. 44, 68 (1967).

¹⁸M. S. Child, J. Mol. Spectrosc. 53, 280 (1974).

¹⁷The results in Refs. 15 and 16 provide connection formulas for one-dimensional problems and, by looking at caustics rather than turning points, could presumably be adapted to two-dimensional cases.

¹⁸To obtain this higher accuracy, the procedure was iterated with three additional trajectories having more decimal places and with values of x(0) and E centered around the trajectory which gave the desired l and n_r . From these three trajectories the value of x(0) and that of E were calculated by interpola-

tion to provide the desired integer values of n_r and l. An additional trajectory was also used with two of the previous trajectories, to calculate as a check, the value of x(0) and E needed to provide the desired integer value of n_r and l, and hence of n and l.

Several tests were performed on the surface of section method. When $p_r < 0$ was chosen instead of $p_r > 0$ the phase integrals $fp_\theta d\theta$ differed only by one part in 20000. The results were also independent of r_0 . The $fp_x dx$ integral had an accuracy of about one part in 10000. The value of the eigenvalue was obtained using different numbers of points and also different trajectories. The precision was better than one part in 5000.

¹⁹For example, in the test of the trajectory closure method against the two surfaces of section method for the state (± 5, 5), the same trajectories used for the (4.1)-(4.2) method were run. The trajectory closure method gave the eigenvalue as 5.9868, while the (4.1)-(4.2) method gave 5.9869, a difference of one part in 60000.

²⁰J. D. Louck and W. H. Shaffer, J. Mol. Spectrosc. 4, 285 (1960).

²¹Using a variational calculation with basis sets of 406 and 595 elements, the eigenvalues were found to be stable up to an energy of 11.0 and to agree to about one part in 10 000 at the higher energies and much better than this at lower energies.

²² EISPAC is a package developed by National Activity to Test Software. See, for example, Lecture Notes in Computer Science, edited by G. Goos and J. Hartman, Vol. 6 (Springer, Berlin, 1976).

²³M. Tinkham, Group Theory and Quantum Mechanics (McGraw-Hill, New York, 1964).

²⁴See, for example, Fig. 2 in J. Ford, Adv. Chem. Phys. 24, 155 (1973).

²⁵See, for example, Fig. 3 in Ref. 24.

²⁶For example, in Eq. (13) and paper II in Ref. 2(c) it is assumed that $\int p_x dx$ is independent of the path. However, the necessary and sufficient condition for this line integral to be independent of the path is that $p_x dx$ be an exact differential. p_x equals $\partial F_2(x, y)/\partial x$, where F_2 is a generating function depending on old variables x and y and on new (constant) momenta. $(\partial F_2/\partial x)dx$ is an exact differential only when F_2 is the sum of a term depending on x alone and a term depending on y alone, i.e., only when the problem is separable. In contrast $p_x dx + p_y dy$ is always an exact differential.

Similarly, Eqs. (23b)—(23c) or I in Ref. 2(o) suppose that because of the $\partial G/\partial q_i$ there is a periodic function of all angle variables q_j , $\int (\partial G/\partial q_i)dq_i$ vanishes over a closed trajectory. However, unless G describes a separable system, $\partial G/\partial q_i$ depends not only on q_i but also on q_j , and the variation of q_j with q_i along a trajectory is not a simple one.

³¹Since the necessary and sufficient condition of separability for the final equations in Ref. 2(o) is not met, we have wondered whether some milder approximation might be used to derive those equations. One possibility is to make the approximation that all velocities of the angle variables q_j satisfy $q_j = q_i N_j/N_i$ throughout the trajectory, where N_j is the number of cycles of the j motion in the closed trajectory. (Clearly they satisfy this equation in some average sense.) One then introduces the fact that $\partial G/\partial q_i$ is a periodic function of the q_j , expands in sines and cosines, and performs the integration. In this way one can derive the final equations of Ref. 2(o), but it should be emphasized that we have introduced an approximation of unknown accuracy, one which should be tested in individual cases.

²⁸R. A. Marcus, Ber. Bunsenges. Phys. Chem. 81, 190 (1977).

²⁹J. D. McDonald and R. A. Marcus, J. Chem. Phys. 64, 2518 (1976).